Talanta 120 (2014) 76–83

Contents lists available at ScienceDirect

Talanta

journal homepage: www.elsevier.com/locate/talanta

A facile approach for imprinting protein on the surface of multi-walled carbon nanotubes

Ren Liu [a], Mo Sha [a], Sisi Jiang [a], Jing Luo [a,b,*], Xiaoya Liu [a,**]

[a] The Key Laboratory of Food Colloids and Biotechnology, Ministry of Education, School of Chemical and Material Engineering, Jiangnan University, Wuxi, Jiangsu 214122, China

[b] State Key Laboratory of Molecular Engineering of Polymers (Fudan University), Shanghai 200433, China

ARTICLE INFO

Article history:
Received 13 July 2013
Received in revised form
29 November 2013
Accepted 2 December 2013
Available online 6 December 2013

Keywords:
Molecular imprinting
MWNTs
Protein
Polydopamine

ABSTRACT

This study describes a green, facile and low cost approach for imprinting protein on the surface of multi-walled carbon nanotubes (MWNTs) using papain as the template, dopamine as the functional monomer. By simply mixing MWNTs, dopamine, template protein in weak alkaline aqueous solution, a thin adherent polydopamine (PDA) film imprinted with protein was spontaneously obtained on the surface of MWNTs to produce the imprinted nanomaterials (MWNTs@MIPs). The obtained MWNTs@MIPs were characterized with Fourier transform infrared spectrometer (FT-IR), Raman spectroscopy, X-ray photoelectron spectroscopy (XPS), scanning electron microscopy (SEM) and transmission electron microscopy (TEM). The adsorption process of the MWNTs@MIPs towards template protein was investigated in detail. The effects of the concentration of the monomer and template, polymerization time, extraction process were optimized. The prepared MWNTs@MIPs show fast binding kinetics, high binding capacity and acceptable specific recognition behavior towards template proteins. Furthermore, the stability and regeneration were also investigated, which indicated that the MWNTs@MIPs had good reusability. The good recognizing behavior coupled to the low cost and facile one-step preparation make the MWNTs@MIPs attractive for separation and specific protein recognition.

1. Introduction

Molecular imprinted polymers (MIPs), described as artificial "locks" for "molecular keys", have the ability to recognize the used template from a mixture of closely related compounds. In other words, recognition sites were generated by polymerizing functional monomer together with the template molecules in the presence of a cross-linking agent. After removing the template molecules, imprinted cavities were left inside the polymer network [1,2]. Owing to their molecular recognition ability, low cost, chemical and mechanical stability, durability, reusability and ease of preparation, MIPs can act as chemical sensors, artificial antibodies, and have been used in separations, enrichments, catalysis, and membrane filtration [3–8].

Despite the attractive features of this technique, MIPs prepared by traditionally bulk polymerization exhibited poor accessibility, low-affinity binding and high diffusion barrier to the template, as the template molecules were embedded inside the thick polymer network. Surface molecular imprinting method provides an alternative way to overcome these drawbacks, which attempts to build molecular recognition systems on the supporting materials surface [9–14]. The advantages of surface molecular imprinting include improving mass transfer, increasing affinity binding and decreasing high diffusion barrier of the template by fixing MIP on a support substrate. Up to now, various materials, such as magnetic nanoparticles [15–21], silica particles [22–24], nanowires/nanotubes [25–28], quantum dots (QDs) [29,30] and polystyrene nanoparticles [31] were chosen to be solid supporting materials for surface molecular printing. Among these materials, multi-walled carbon nanotubes (MWNTs), possessing extraordinarily large specific surface area as well as good mechanical properties, have been proven to be an available support material in surface imprinting process [32–39]. A special tip for fabricating a MIP on the surface of MWNTs was reported by several groups [34–39], in which vinyl groups were introduced onto the MWCNTs surface via covalent or non-covalent method to direct the selective polymerization of functional monomers and cross-linkers in the presence of the template. Another report introduced amine group on the surface of carbon nanotubes to fabricate an oleanonic-imprinted layer on the carbon nanotubes (CNTs) [32]. However, the introduction of double bond or amine group to the surface of carbon

* Corresponding author at: The Key Laboratory of Food Colloids and Biotechnology, Ministry of Education, School of Chemical and Material Engineering, Jiangnan University, Wuxi, Jiangsu 214122, China. Tel./fax: +86 510 8591 7763.

** Corresponding author.

E-mail addresses: jingluo19801007@126.com (J. Luo), lxy@jiangnan.edu.cn (X. Liu).

0039-9140/$ - see front matter © 2013 Elsevier B.V. All rights reserved.
http://dx.doi.org/10.1016/j.talanta.2013.12.002

nanotubes often involves harsh conditions and/or multiple reaction steps. In addition, the polymerization was mostly carried out in organic solvent at high temperatures, which is quite a disadvantage for imprinting biological molecules. Therefore, new approaches for the molecular imprinting on the surface of MWNTs are still highly desired.

On the other hand, while MIPs have been successfully developed against a wide range of small molecules, the imprinting of biomacromolecules, such as proteins, remains a challenge. The major difficulties associated with the imprinting of biomacromolecules include (i) the insolubility of proteins in commonly utilized imprinting solvents, (ii) the degradation of proteins under polymerization conditions such as high temperature, (iii) the large molecular size and structural complexity which restrict their mobility [8]. Surface imprinting is quite attractive for imprinting protein because the imprinted sites are close to or at the surface of MIP avoiding the protein entrapment in the polymer matrix and so enable the elution and rebinding of the target protein easily. However, as far as we are aware, no one has reported the imprinting of protein on the surface of MWNTs.

In recent years, the self-polymerization of dopamine on a wide variety of materials in aqueous solution to form polydopamine (PDA) coatings has been reported [40,41]. The resulted PDA film has a crosslinked structure to generate stable three-dimensional recognition sites. The thickness of the PDA film, which decides the depth of the imprinted cavities, is in nanoscale range and could be adjusted by changing the polymerization time. In addition, its multifunctional groups (amino and catechol groups), hydrophilicity and biocompatibility make it appropriate for imprinting bimacromolecules [42]. Several successful examples of employing PDA in molecular imprinting have been published [43–47].

Considering the advantages of MWNTs and PDA, the key idea of this paper is to develop a facile approach to imprint protein on the surface of MWNTs using dopamine as monomer. Just by mixing MWNTs, dopamine, template protein in weak alkaline aqueous solution, a thin adherent polydopamine (PDA) film imprinted with protein was spontaneously obtained on the surface of MWNTs to produce the imprinted nanomaterial (MWNTs@MIPs). This one-pot procedure avoids the surface-modification of MWNTs, representing a rapid, efficient and green approach to fabricate protein imprinted nanomaterials. The adsorption dynamics, special adsorption, and selective recognition of the MWNTs@MIPs were investigated. The results show that MWNTs@MIPs possess high rebinding capacity, specific recognition ability and good recycle performance towards template protein (papain) in aqueous media.

2. Experimental

2.1. Reagents and apparatus

MWNTs were purchased from Chengdu Organic Chemicals Co. Ltd. of Chinese Academy of Sciences. Dopamine hydrochloride (DA), papain (Pap), bovine serum albumin (BSA), lysozyme (Lyz), egg albumin and horseradish (HRP) were purchased from the Shanghai Alladin Chemical Reagent Company. All other chemicals were of analytical grade and used as received without further purification except for special statement. Doubly distilled water was used throughout the work.

UV–vis spectra were recorded on a TU-1901 spectro-photometer (Beijing Purkinje General Instrument Co., Ltd.). Raman was recorded with a Renishaw in via Raman Microscope operating at 514 nm with a charge-coupled device detector. XPS measurement was made on a VG ESCALAB MkII spectrometer with a Mg–Ka X-ray source (1253.6 eV photos). The X-ray source was operated at 14 kV and 20 mA. The morphologies of samples were determined using scanning electron microscopy (SEM) (Hitachi S-3700 N, Tokyo, Japan). TEM measurements were carried on a JEOL JEM-2100 microscope operating at 200 KV. Thermal gravimetric analysis (TGA) was conducted on a SDT 2960 instrument from room temperature to 850 °C with a heating rate of 20 °C min^{-1} in the nitrogen flow (10 mL min^{-1}). Gel electrophoresis for protein separation was carried out by regular sodium dodecyl sulfate polyacrylamide gel electrophoresis (SDS-PAGE) with 12% running gel and 5% stacking gel according to the manual introduction (Bio-Rad, Hercules, CA, USA). Proteins were stained with Coomasie Brilliant Blue R-250.

2.2. Preparation of MWNTs@MIPs

In a typical MWNTs@MIPs synthesis, MWNTs (20 mg) was dispersed in 20 mL Tris buffer (pH 8.0) by ultrasonication. 5 mg of papain and 16 mg of DA were then added. The mixture was stirred for 8 h at room temperature. After reaction, the product was washed with water to remove the unreacted monomer, then washed with a mixture of acetic acid (0.6 mol/L) and methanol (the ratio between acetic acid and methanol is 1:4, v/v) to extract the template protein and re-washed thoroughly with distilled water. For comparison, non-imprinted materials (MWNTs@NIPs) were prepared and treated under the same conditions but without the addition of the template protein.

2.3. Adsorption experiment of MWNTs@MIPs and MWNTs@NIPs

All the binding experiments were carried out in glass vials by using a batch technique. Before binding experiments, a calibration curve was obtained from the UV–vis spectra of the papain solutions with different concentrations. MWNTs@MIPs (10 mg) or MWNTs@NIPs (10 mg) was suspended in 10 mL papain solutions of different concentrations. The sample was incubated on a rocking table for 40 min at room temperature, then the mixture was centrifuged and the supernatant solution was collected. The concentration of free papain in the supernatant was measured by UV–vis at 276 nm. The papain bound was expressed as the difference between the total mass of papain loaded and mass of papain in solution after binding. The adsorption dynamics of the MWNTs@MIPs was performed by analyzing the free papain concentration in the supernatant at different time intervals.

2.4. Selectivity experiments

In the selectivity experiments, bovine serum albumin (BSA), lysozyme (Lyz), egg albumin were chosen as the reference substrates to investigate the selectivity to the template protein. For the separative adsorption experiments, the different protein solutions (each with a concentration of 0.3 mg mL^{-1}) were applied to bind with the imprinted and non-imprinted materials respectively. The resulting concentrations of BSA, Lyz, and albumin in the supernatant were measured by the UV–vis separatively. For the mixed adsorption experiments, Lyz and HRP were chosen as the competitive protein. The adsorption was performed within a protein mixture (containing papain, Lyz and HRP). Ten microliter of the mixed solution, before and after the adsorption, was extracted for SDS-PAGE analysis.

3. Results and discussion

3.1. Preparation and characterization of papain imprinted MWNTs@MIPs

Fig. 1 depicts the schematic representation of MWNTs@MIPs preparation. A simple mixture of MWNTs and dopamine in a weak

alkaline solution containing papain (Tris buffer, pH 8.0) resulted in the self-polymerization of DA and spontaneous deposition of a thin adherent PDA layer on MWNTs surface. During this process, the template proteins were embedded in the PDA film since its molecules can interact with dopamine units. As there are a lot of amine and hydroxyl groups in the PDA chain, these groups provide multifunctional binding sites to template molecules by hydrogen and π–π bonds, which is favorable for obtaining high imprinting and rebinding efficiency. This imprinting process creates a micro-environment for the recognition of protein based on shape selection and functional group positioning. Finally, the papain molecules were removed from the PDA layer by washing, leading to the preparation of papain imprinted MWNTs@MIPs composite.

An insight into the surface morphology of the modified surface of MWNTs@MIPs composite was feasible through SEM and TEM images. As shown in Fig. 2, the pristine MWNTs showed clearly visible nanotubes, and the MWNTs@MIPs composite also exhibited nanowire morphology. However, the average diameter of MWNTs@MIPs composite was much larger than that of MWNTs, indicating that the PDA layer was attached on the MWNTs successfully. In addition, the MWNTs@MIPs exhibited a slightly rough surface compared to pristine MWNTs, which may assist papain to be rebinded rapidly. The detailed morphology of the printine MWNTs and MWNTs@MIPs composite was captured by TEM. From the TEM images (Fig. 3A), the average thickness of wall and length of the crude MWNTs were about 20 nm and several micrometers, respectively. For MWNTs@MIPs composite (Fig. 3B), a PDA layer with well defined shape and configuration was readily observed on the MWNTs surface with light contrast. In addition, the diameter of the MWNTs@MIPs nanocomposite was increased to 50–60 nm after the imprinting process, which corresponds to a roughly 15–20 nm thick imprinted PDA layer covered on MWNTs. The thickness of the imprinted polymer layer was 15–20 nm, which would be effective to the mass transport between solution and the surface of MWNTs.

Fig. 4A compared the FTIR spectra of the pristine MWNTs and MWNTs@MIPs. For MWNTs@MIPs, the strong peaks at 1627 and 1543 cm^{-1}, corresponding to the typical absorption peaks of phenyl group on PDA chain, was observed [44]. The broad band between 2800 and 3400 cm^{-1} which can be attributed to the stretching vibration of –OH (phenolic hydroxyl) or $-NH_2$ on PDA chain, were also found for MWNTs@MIPs sample. The above peaks proved the formation of PDA film on the surface of MWNTs.

The presence of PDA layer on the surface of MWNTs was further investigated by the TGA data. Fig. 4B showed TGA weight loss curves of crude MWNTs and MWNTs@MIPs composites, respectively. As shown in curve *a*, the crude MWCNTs were stable without weight loss below 600 °C. In comparison, the MWNTs@MIPs started to decompose at 290 °C and a 25% weight loss occurred in the same temperature range, which was thus undoubtedly assigned to the thermal degradation of the PDA layer. Fig. 4C showed the Raman spectra of MWNTs and MWNTs@MIPs. Two characteristic peaks centered at about 1352 and 1582 cm^{-1}, corresponding to the D and G bands of the MWNTs [49], were observed in both samples. However, compared with the pristine MWNTs, the frequencies of the D and G bands of MWNTs@MIPs were red-shifted about 2–3 cm^{-1}. Additionally, the ratio values of I_D/I_G of MWNTs were decreased from 2.2 to 1.5 of MWNTs@MIPs. Raman results further indicated that the PDA layer was successfully introduced onto the surface of MWNTs.

The surface chemical structure of the MWNTs@MIPs was measured by XPS. The elements including carbon (C), oxygen (O), and nitrogen (N) were confirmed by a survey XPS scan ranging from 0 to 1200 eV (Fig. 4D). Evidently, there is no nitrogen signal detected for MWNTs (curve a). While, in the case of the MWNTs@MIPs, the N1s peak appears at 399.5 eV (curve b), which belongs to the nitrogen element of amino groups in the polydopamine chain, demonstrating successful formation of PDA polymer layer on MWNTs surface. Additionally, the ratio of nitrogen to carbon (N/C) peak areas was 0.11, which was near

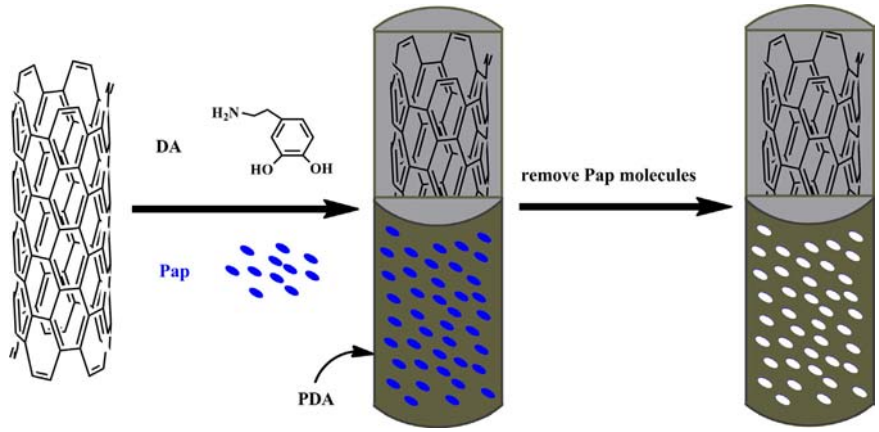

Fig. 1. Schematic illustration of the preparation of MWNTs@MIPs.

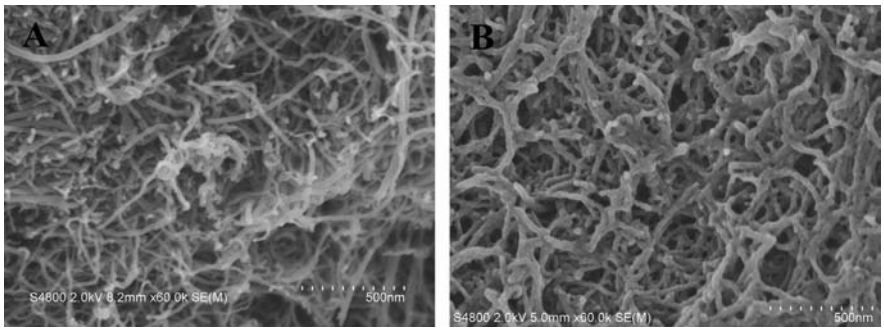

Fig. 2. The SEM image of MWNTs (A) and MWNTs@MIPs (B).

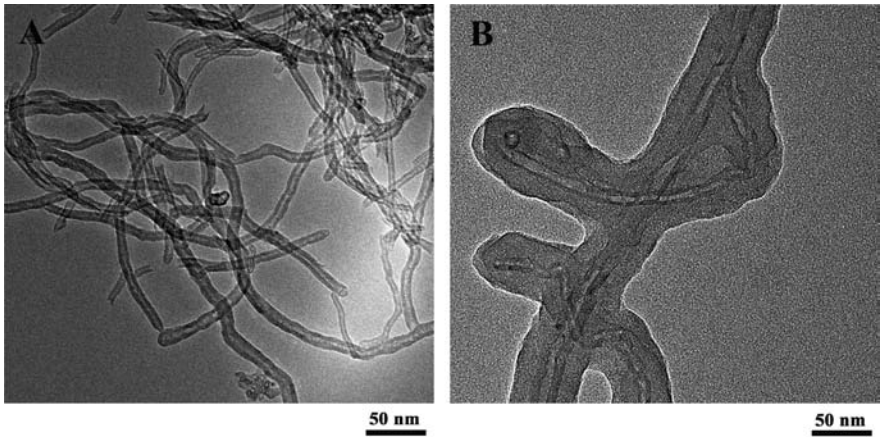

Fig. 3. The TEM image of MWNTs (A) and MWNTs@MIPs (B).

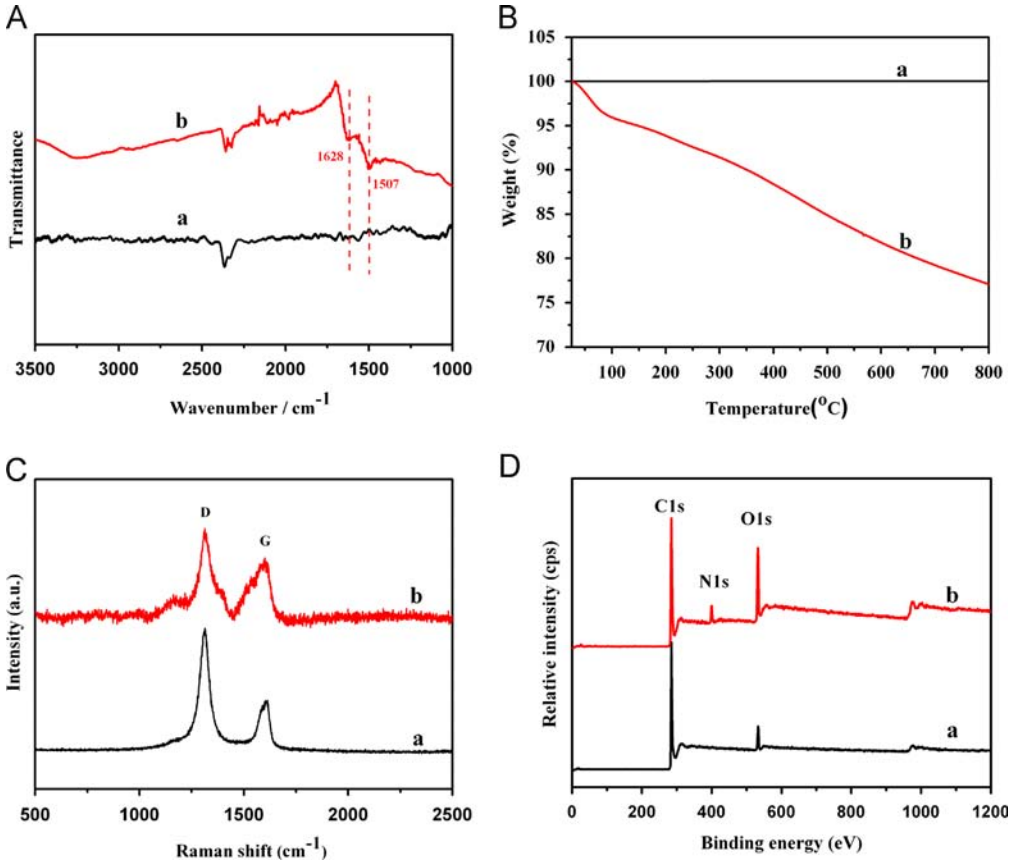

Fig. 4. Characterization of MWNTs (a) and MWNTs@MIPs (b). (A) FT-IR spectra, (B) TGA, (C) Raman spectra, and (D) XPS spectra.

to the theoretical value of 0.125 of DA [48], indicating that MWNTs has been completely coated by PDA polymer shell.

The PDA layer on the MWNTs surface also provided a hydrophilic surface and thus high dispersibility in water. Dispersion of crude MWNTs in water is difficult and the MWNTs quickly precipitated within 15 min. In the sharp contrast, after surface modification with PDA layer, MWNTs@MIPs could be well-dispersed in water over several days, suggesting that the hydrophilic PDA layer was successfully conjugated on the surface of MWNTs.

3.2. Optimization of the MWNTs@MIPs preparation conditions

In order to determine the most favorable conditions for synthesizing the MWNTs@MIPs, different influencing factors, such as the concentration of functional monomer (DA) and template protein (papain), polymerization time and extraction conditions were investigated on the adsorption capacity of the MWNTs @MIPs composites. The adsorption capacity was obtained from the adsorption experiments.

(a) Monomer concentration. Different concentrations of DA ranging from 0.2 to 1.2 mg/mL were applied in the preparation of MWNTs@MIPs. As shown in Fig. 5A, the binding amount of the resulting MWNTs@MIPs toward template protein increased with increasing monomer DA concentration and reached a maximum binding amount at 0.8 mg/mL. We presume that increasing DA amount could increase the thickness of PDA film on the surface of MWNTs, which can accommodate more

papain molecule and thus lead to the increase in the number of recognition cavities. When the DA concentration was higher than 0.8 mg/mL, the further increasing thickness of the PDA layer blocked the site accessibility and led to the decrease in the binding amount of template protein.

(b) Template protein concentration. Similarly, the effect of template protein concentration was also investigated in the range from 0.1 to 0.3 mg/mL and the results are given in Fig. 5B. The binding amount for papain increased with increasing template molecule concentration due to the increase in the number of recognition cavities. A maximum binding amount was achieved at the papain concentration of 0.25 mg/mL.

(c) Reaction time. In order to create more imprinted sites and get rapid response, the PDA film thickness on MWNTs surface was adjusted via controlling reaction time. As shown in Fig. 5C, the binding amount for papain increased remarkably with the increasing polymerization time. The optimal recognition performance toward papain was achieved at 8 h. Further extending the reaction time led to decrease in the binding amount, which may be due to that longer time would increase the thickness of the PDA film on the surface of MWCNT, and thus led to poor site accessibility of imprinted cavities for template protein.

(d) Extraction time. In our work, a mixture of acetic acid (0.6 mol/L) and methanol (the ratio between acetic acid and methanol is 1:4, v/v) was used to extract the template molecules from the PDA layer. With the extraction going on, more and more template molecules were extracted from the PDA layer, leading to an increasing number of imprinted cavities and thus increase in the rebinding amount of template protein. As shown in Fig. 5D, at the extracting time of 4 h, the rebinding amount reached the maximum value. With prolonging extraction time, the imprinted cavities may be partly destroyed.

3.3. Recognition properties of the MWNTs@MIPs

The kinetic binding behavior of MWNTs@MIPs was evaluated by studying the absorption toward papain at different time. Fig. 6 shows the relationship between the adsorption capacity and the time. We can see that the MWNTs@MIPs reached adsorption equilibrium at 35 min and the adsorption process before equilibrium can be divided into two steps: rapid increases within the first 15 min and then levels off as equilibrium reached. In contrast, previous reported imprinted materials often required more than 2 h to achieve the adsorption equilibrium. Thus the rebinding rate of our MWNTs@MIPs is quite fast, which is attributed to that the thickness of MIPs layer on the surface of MWNTs is in the nanometer range, making the recognition sites accessible for the template molecules. Thus, the papain molecules could reach the surface imprinting cavities easily and took less time to reach adsorption equilibrium.

In order to investigate the binding performance of MWNTs@MIPs against control MWNTs@NIPs, an equilibrium binding analysis experiment was carried out. Protein papain solutions with concentrations ranging from 0.1 to 0.45 mg mL^{-1} were prepared in 0.05 M tri-buffer. After 40 min incubation, which was sufficient to reach the equilibrium of absorption, the solutions were separated and the concentrations of the solutions were measured. Fig. 7 shows the adsorption isotherms of MWNTs@MIPs and the control MWNTs@NIPs at different initial concentrations of papain. It can be clearly observed that the MWNTs@MIPs exhibited a higher binding capacity than that of the MWNTs@NIPs. The weak adsorption of papain to the MWNTs@NIPs may be attributed to the non-specific interaction with the polymer matrix. In addition, with increasing initial concentration of papain, the absorption amount of MWNTs@MIPs toward papain increased and reached maximum at the concentration of 0.3 mg/mL. MWNTs@NIPs exhibited the same trend as MWNTs@MIPs with a

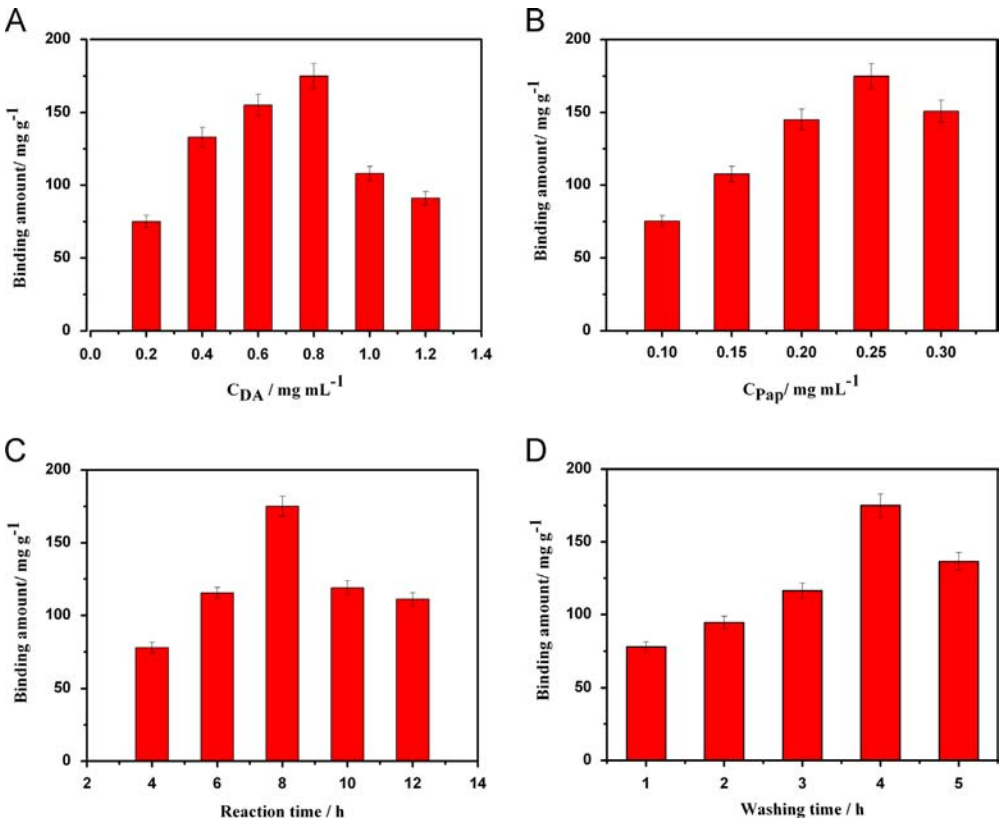

Fig. 5. Effect of the concentration of DA (A) and papain (B), reaction time (C), washing time (D) on the recognition behavior of the MWNTs@MIPs towards papain. The points represent mean values of three measurements.

lower saturated adsorption amount. The maximum absorption capacities are calculated to be 175 mg/mL for MWNTs@MIPs, much higher than 72 mg/mL for MWNTs@NIPs. The result could be explained by the fact that the imprinting process in preparing MWNT@MIPs could form specific recognition cavities which fit the size and shape of the template molecule and thus showed specific affinity for papain. In contrast, in the case of MWNT@NIPs, the non-specific adsorption had a dominant effect due to lack of recognition sites. Therefore, the binding capacity of papain was low.

Selective recognition toward the template molecule, which is based on the imprinted cavities complement to the size, shape, and functionality of the template molecule, is an important property for imprinted material. In order to verify that MWNT@MIPs is selective to papain, three other proteins were chosen as the comparative substrates. In a typical procedure, the MWNT@MIPs was added to 0.05 M tris buffer containing 0.3 mg/mL papain, Lyz, BSA and egg albumin, respectively. The protein concentrations were measured after 40 min incubation at room temperature. The same experiments were carried out with MWNT@NIPs. Fig. 8 showed the rebinding capacities of the MWNT@MIPs and MWNT@NIPs for these proteins. It can be observed that the amount of papain adsorbed onto the MWNT@MIPs was obviously higher than those of the other proteins. In addition, the imprinting factor α (the amounts of papain bound by MWNT@MIPs/the amounts of papain bound by MWNT@NIPs), which measures the imprinting effect, is 2.5 for binding papain, much higher than those toward the competetive proteins studied, where α of Lyz, BSA and egg albumin were 1.4, 1.2 and 1.15, respectively. These results demonstrated that the MWNT@MIPs had specific recognition toward the imprinted protein.

To further illustrate the recognition behavior of the MWNTs @MIPs, binary protein competitive binding experiments were also performed. BSA, Lyz and egg albumin were used as competitors in the coexistence of equivalent template protein. As shown in Fig. 9, in the presence of BSA, Lyz and egg albumin, the relative rebinding of papain to MWNTs@MIPs reached about 87%, 81% and 90%, respectively. The comparatively lower rebinding in the presence of Lyz is attributed to the small size of Lyz, which resulted in more non-specific adsorption. Furthermore, even in the presence of higher concentration of nontemplate proteins than the concentration of papain, the relative binding of papain still reached about 70–80%.

The above results demonstrated the high specificity and selectivity of the MWNTs@MIPs toward template proteins, which was attributed to the selective fitting of papain molecules into complementary cavities created in the MWNT@MIPs during the imprinting procedure. The selective fitting involves two roles: the shape complementary cavity structure just fitting for the unique structure of papain; synergistic effects of multiple interactions provided by the polydopamine such as amino-containing, hydroxyl-containing groups and π–π bonds as well as van der Waals forces available for interaction with the template protein.

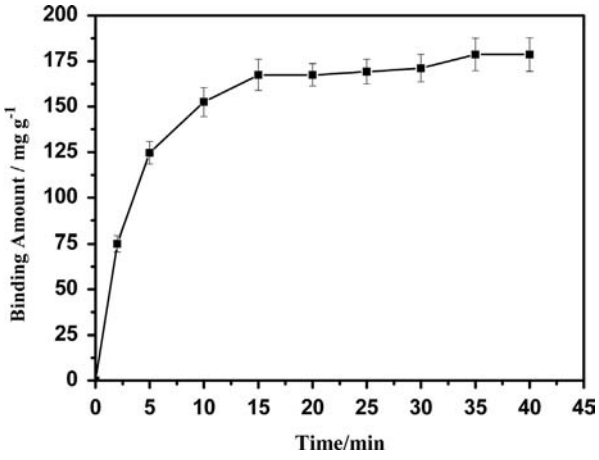

Fig. 6. Adsorption kinetics of papain on MWNTs@MIPs. 20 mg sample of MWNTs@MIPs was incubated in a solution of papain at a concentration of 0.30 mg/mL at 25 °C. The points represent mean values of three measurements.

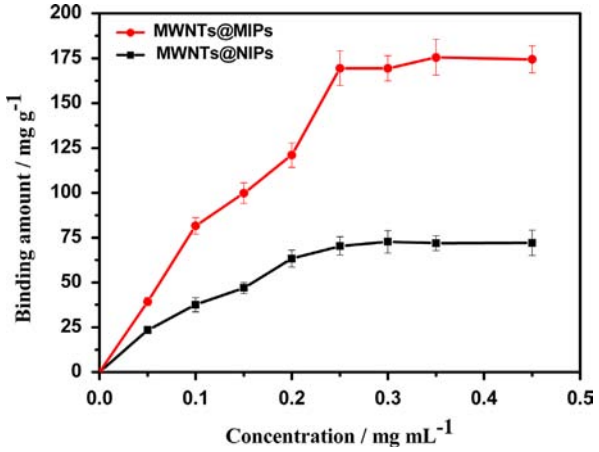

Fig. 7. Adsorption isotherms of papain on MWNTs@MIPs and MWNTs@NIPs. The concentration of MWNTs@MIPs and MWNTs@NIPs was 1 mg/mL. The points represent mean values of three measurements.

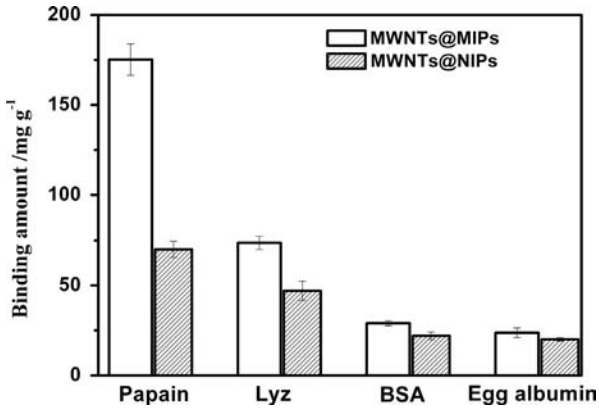

Fig. 8. Binding amount of different proteins on MWNTs@MIPs and MWNTs@NIPs. The initial template papain and nontemplate protein concentration used for binding was 0.3 mg/mL. The concentration of MWNTs@MIPs and MWNTs@NIPs was 1 mg/mL. The points represent mean values of three measurements.

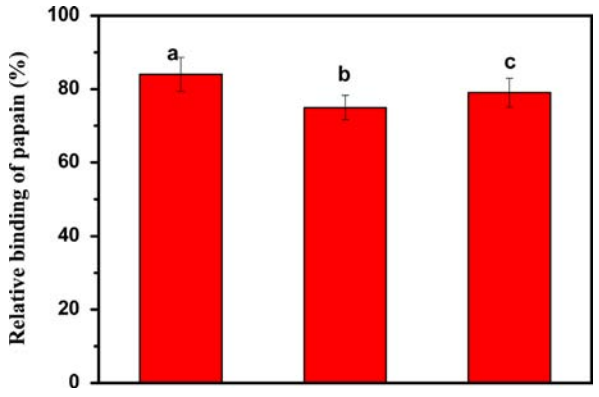

Fig. 9. Competitive binding of template papain with non-template (a) HRP, (b) Lyz and (c) egg albumin. The initial template papain and nontemplate protein concentration used for binding was 0.3 mg/mL. The concentration of MWNTs@MIPs was 1 mg/mL. The points represent mean values of three measurements.

3.4. Selective separation of papain from protein mixtures and real sample adsorption

The selectivity of MWNTs@MIPs toward template protein was compared by the isolation of Lyz from model protein mixtures, which contained 0.25 mg/mL papain, 0.25 mg/mL Lyz and 0.6 mg/mL HRP. A mass of 30 mg imprinted and non-imprinted materials were tested respectively. The result of SDS-PAGE analysis for the mixture solution was shown in Fig. 10. There were three bands in the lane 1, indicating the mixture of papain, Lyz and HRP. After treatment with MWNTs@MIPs, it was found that the band of papain faded noticeably while the band of Lyz and HRP had little change (lane 2), suggesting most of the papain was selectively captured by MWNTs@MIPs and the high specificity of MWNTs@MIPs toward the template. Different from lane 3, still three bands were observed in lane 3, including papain, Lyz and HRP, after treatment with MWNTs@NIPs. The result further validated that MWNTs@NIPs had no selectivity toward papain.

The practicability of MWNTs@MIPs was demonstrated by selective removal and enrichment of papain from a commercially available meat tenderizer, where aqueous solution of meat tenderizer was spiked with 0.25 mg mL^{-1} papain. Meat tenderizer was chosen as the real sample as papain is frequently used to prepare meat tenderizer [49]. The result of SDS-PAGE analysis for the solution of meat tenderizer before and after the adsorption was demonstrated in Fig. 11. It could be clearly seen that the intensity of the papain band was significantly weaker (lane 2) after treatment with MWNTs@MIPs. The band of papain reappeared and became dark (lane 3) upon SDS-PAGE analysis of the eluted solution of the absorbed papain, suggesting that papain was well isolated and enriched after elution. The above results confirmed the practicability of the MWNTs@MIPs for the selective isolation and enrichment of papain.

3.5. Reproducibility and regeneration of MWNTs@MIPs

Desorption and regeneration is one of the most important properties for the application of the MWNTs@MIPs. The MWNTs@MIPs could be regenerated after washing with a mixture of acetic acid (0.6 mol/L) and methanol (the ratio between acetic acid and methanol is 1:4, v/v). To investigate the stability and regeneration of the MWNTs@MIPs, the adsorption–desorption cycle was repeated four times using the same

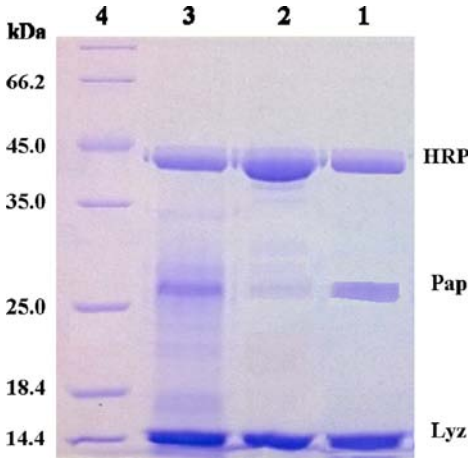

Fig. 10. SDS-PAGE analysis of spiked protein mixture treated with MWNTs@MIPs and MWNTs@NIPs. Lane (1)—spiked protein mixture (0.25 mg/mL papain, 0.25 mg/mL Lyz and 0.6 mg/mL HRP); (2)—the supernatant after treatment with MWNTs@MIPs; (3)—the supernatant after treatment with MWNTs@NIPs; (4)—marker. Loading amount of protein mixture: 10 μL. Lyz: lysozyme; Pap: papain; HRP: horseradish.

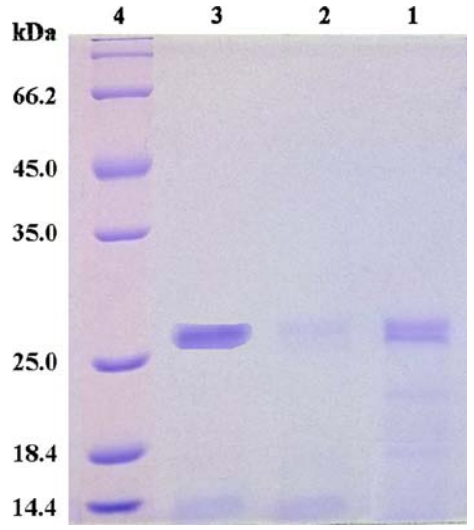

Fig. 11. SDS-PAGE analysis of meat tenderizer solution before and after treatment with MWNTs@MIPs. Lane (1) meat tenderizer solution; (2) the supernatant after treatment with MWNTs@MIPs; (3) the eluate from lane 2; (4) marker; and loading amount of sample: 10 μL.

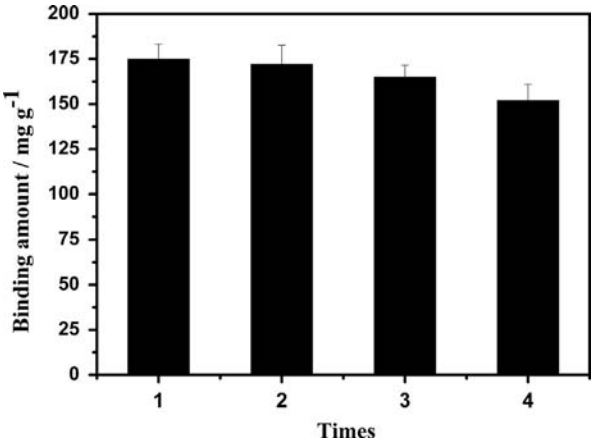

Fig. 12. Stability and regeneration of the MWNTs@MIPs. The initial template papain used for binding was 0.3 mg/mL. The concentration of MWNTs@MIPs was 1 mg/mL. The points represent mean values of three measurements.

MWNTs@MIPs sample. As shown in Fig. 12, the MWNTs@MIPs were stable up to 4 adsorption cycles with only a little decrease in the binding capacity. The possible reason for the decrease in absorption is that some recognition cavities in the PDA layer might be deformed during the regeneration process, and thus they no longer matched the template molecules. The loss of MWNTs@MIPs from the centrifugation process may also contribute to the decrease in adsorption capacity.

4. Conclusion

Herein, in this work, we have developed a facile approach to imprint protein based on surface coating of MWNTs with a thin layer of PDA polymerized in the presence of protein templates. Compared to previous methods, this approach avoids the surface-modification of MWNTs and is carried out in aqueous solution at ambient temperature, representing a rapid, efficient and green approach to fabricate protein imprinted nanomaterials. The obtained MWNTs@MIPs exhibited fast adsorption kinetics, high binding capacity, significant selectivity and good reproducibility. All these results

demonstrated that have potential in the separation and recognition of biomacromolecules.

Acknowledgment

We acknowledge financial support from the National Natural Science Foundation of China (under Grant nos. 51103064 and 21174056), the Fundamental Research Funds for the Central Universities (JUSRP51305A), the Open Project Program of the State Key Laboratory of Molecular Engineering of Polymers (K2012–04) and the Program for the New Century Excellent Talents in University (NCET-10-0452).

References

[1] G. Wulff, Chem. Rev. 102 (2001) 1–28.
[2] F.G. Tamayo, A. Martin-Esteban, J. Chromatogr. A 1098 (2005) 116–122.
[3] B. Sellergren, R.N. Karmalkar, K.J. Shea, J. Org. Chem. 65 (2000) 4009–4027.
[4] E.L. Holthoff, F.V. Bright, Anal. Chim. Acta 594 (2007) 147–161.
[5] K. Haupt, K. Mosbach, Chem. Rev. 100 (2000) 2495–2504.
[6] L. Ye, K. Mosbach, Chem. Mater. 20 (2008) 859–868.
[7] V. Suryanarayanan, C.T. Wu, K.C. Ho, Electroanalysis 22 (2010) 1795–1811.
[8] Y. Li, T. Tan, F. Svec, Biotechnol. Adv. (2013).
[9] D.R. Kryscio, N.A. Peppas, Anal. Chim. Acta 718 (2012) 109–115.
[10] J.X. Liu, K.G. Yang, Q.L. Deng, Q.R. Li, L.H. Zhang, Z. Liang, Y.K. Zhang, Chem. Commun. 47 (2011) 3969–3971.
[11] M.S. Zhang, J.R. Huang, P. Yu, X. Chen, Talanta 81 (2010) 162–166.
[12] W. Zhang, L. Qin, X.W. He, W.Y. Li, Y.K. Zhang, J. Chromatogr. A 1216 (2009) 4560–4567.
[13] B.J. Gao, H.Y. Fu, Y.B. Li, R.K. Du, J. Chromatogr., B: Anal. Technol. Biomed. Life Sci. 878 (2010) 1731–1738.
[14] O. Hayden, C. Hadersp€ock, S. Krassnig, X.H. Chen, F.L. Dickert, Analyst 131 (2006) 1044–1050.
[15] L. Li, X.W. He, L.X. Chen, Y.K. Zhang, Chem.–Asian J. 4 (2009) 286–293.
[16] X.W. Kan, Q. Zhao, D.L. Shao, Z.R. Geng, Z.L. Wang, J.J. Zhu, J. Phys. Chem. B 114 (2010) 3999–4004.
[17] Q.Q. Gai, F. Qu, Z.J. Liu, R.J. Dai, Y.K. Zhang, J. Chromatogr., A 1217 (2010) 5035–5042.
[18] W.H. Zhou, C.H. Lu, X.C. Guo, F.R. Chen, H.H. Yang, X.R. Wang, J. Mater. Chem. 20 (2010) 880–883.
[19] M. Zhang, X.H. Zhang, X.W. He, L.X. Chen, Y.K. Zhang, Nanoscale 4 (2012) 3141–3147.
[20] R.X. Gao, X. Kong, X. Wang, X.W. He, L.X. Chen, Y.K. Zhang, J. Mater. Chem. 21 (2011) 17863–17871.
[21] T. Jing, H.R. Du, Q. Dai, H. Xia, J.W. Niu, Q.L. Hao, S.R. Mei, Y.K. Zhou, Biosens. Bioelectron. 26 (2010) 301–306.
[22] W. Cheng, Z. Liu, Y. Wang, Talanta 116 (2013) 396–402.
[23] G.Q. Fu, H.Y. He, Z.H. Chai, H.C. Chen, J. Kong, Y. Wang, Y.Z. Jiang, Anal. Chem. 83 (2011) 1431–1436.
[24] Z. Lin, Z. Xia, J. Zheng, D. Zheng, L. Zhang, H. Yang, G. Chen, J. Mater. Chem. 22 (2012) 17914.
[25] M.S. Zhang, J.R. Huang, P. Yu, X. Chen, Talanta 81 (2010) 162–166.
[26] Y. Li, H.H. Yang, Q.H. You, Z.X. Zhuang, X.R. Wang, Anal. Chem. 78 (2006) 317–320.
[27] T. Chen, M.W. Shao, H.Y. Xu, S.J. Zhou, S.S. Liu, S.T. Lee, J. Mater. Chem. 22 (2012) 3990–3996.
[28] R.Z. Ouyang, J.P. Lei, H.X. Ju, Chem. Commun. (2008) 5761–5763.
[29] W. Zhang, X.W. He, W.Y. Li, Y.K. Zhang, Chem. Commun. (2012) 1757–1759.
[30] W. Zhang, X.W. He, Y. Chen, W.Y. Li, Y.K. Zhang, Biosens. Bioelectron. 26 (2011) 2553–2558.
[31] C.J. Tan, S. Wangrangsimakul, R.B. Bai, Y.W. Tong, Chem. Mater. 20 (2008) 118–127.
[32] X. Chen, Z.H. Zhang, X. Yang, J.X. Li, Y.N. Liu, H.J. Chen, W. Rao, S.Z. Yao, Talanta 99 (2012) 959–965.
[33] X. Kan, H. Zhou, C. Li, A. Zhu, Z. Xing, Z. Zhao, Electrochim. Acta 63 (2012) 69–75.
[34] X. Kan, Y. Zhao, Z. Geng, Z. Wang, J. Zhu, J. Phys. Chem. C 112 (2008) 4849–4854.
[35] P.Y. Chen, P.C. Nien, C.W. Hu, K.C. Ho, Sens. Actuators B 146 (2010) 466–471.
[36] B.B. Prasad, R. Madhuri, M.P. Tiwari, P.S. Sharma, Electrochim. Acta 55 (2010) 9146–9156.
[37] B. BaliPrasad, A. Prasad, M.P. Tiwari, Biosens. Bioelectron. 39 (2013) 236–243.
[38] D. Zhang, D. Yu, W. Zhao, Q. Yang, H. Kajiura, Y. Li, T. Zhou, G. Shi, Analyst 137 (2012) 2629.
[39] X.L. Zhang, Y. Zhang, X.F. Yin, B.B. Du, C. Zheng, H.H. Yang, Talanta 105 (2013) 403–408.
[40] B. Yu, D.A. Wang, Q. Ye, F. Zhou, W.M. Liu, Chem. Commun. (2009) 6789–6791.
[41] M.E. Lynge, R. Westen, A. Postmab, B. St€adler, Nanoscale 3 (2011) 4916–4928.
[42] H. Lee, S.M. Dellatore, W.M. Miller, P.B. Messersmith, Science 318 (2007) 426–430.
[43] R.Z. Ouyang, J.P. Lei, H.X. Ju, Chem. Commun. (2008) 5761–5763.
[44] M. Zhang, X. Zhang, X. He, L. Chen, Y. Zhang, Nanoscale 4 (2012) 3141–3147.
[45] X. Jia, M. Xu, Y. Wang, D. Ran, S. Yang, M. Zhang, Analyst 138 (2013) 651–658.
[46] W.H. Zhou, C.H. Liu, X.C. Guo, F.R. Chen, H.H. Yang, X.R. Wang, J. Mater. Chem. 20 (2010) 880–883.
[47] T. Chen, M.W. Shao, H.Y. Xu, S.J. Zhuo, S.S. Liu, S.T. Lee, J. Mater. Chem. 22 (2012) 3990–3996.
[48] J.W. Cui, Y.J. Wang, A. Postma, J.C. Hao, L. Rigau, F. Caruso, Adv. Func. Mater. 20 (2010) 1625–1631.
[49] C.K. Kang, W.D. Warner, J. Food Sci. 39 (1974) 812–818.